Research Article

NEURAL REGENERATION RESEARCH
www.nrronline.org

Peripheral nerve fibroblasts secrete neurotrophic factors to promote axon growth of motoneurons

https://doi.org/10.4103/1673-5374.332159

Date of submission: June 11, 2021

Date of decision: September 15, 2021

Date of acceptance: November 9, 2021

Date of web publication: January 7, 2022

Qian-Ru He#, Meng Cong#, Fan-Hui Yu, Yu-Hua Ji, Shu Yu, Hai-Yan Shi, Fei Ding*

From the Contents

Graphical Abstract *Brain-derived neurotrophic factor secreted from nerve fibroblasts (N-Fbs) increases the expression of β-actin and F-actin through the ERK and AKT pathways and enhances motoneuron neurite outgrowth*

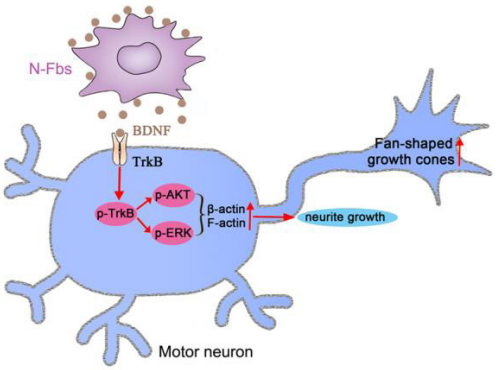

Abstract

Peripheral nerve fibroblasts play a critical role in nerve development and regeneration. Our previous study found that peripheral nerve fibroblasts have different sensory and motor phenotypes. Fibroblasts of different phenotypes can guide the migration of Schwann cells to the same sensory or motor phenotype. In this study, we analyzed the different effects of peripheral nerve-derived fibroblasts and cardiac fibroblasts on motoneurons. Compared with cardiac fibroblasts, peripheral nerve fibroblasts greatly promoted motoneuron neurite outgrowth. Transcriptome analysis results identified 491 genes that were differentially expressed in peripheral nerve fibroblasts and cardiac fibroblasts. Among these, 130 were significantly upregulated in peripheral nerve fibroblasts compared with cardiac fibroblasts. These genes may be involved in axon guidance and neuron projection. Three days after sciatic nerve transection in rats, peripheral nerve fibroblasts accumulated in the proximal and distal nerve stumps, and most expressed brain-derived neurotrophic factor. *In vitro*, brain-derived neurotrophic factor secreted from peripheral nerve fibroblasts increased the expression of β-actin and F-actin through the extracellular regulated protein kinase and serine/threonine kinase pathways, and enhanced motoneuron neurite outgrowth. These findings suggest that peripheral nerve fibroblasts and cardiac fibroblasts exhibit different patterns of gene expression. Peripheral nerve fibroblasts can promote motoneuron neurite outgrowth.

Key Words: brain-derived neurotrophic factor; differential gene expression; F-actin; fibroblasts; motoneurons; mRNA sequencing; neurite outgrowth; peripheral nervous system; β-actin

Introduction

Peripheral nerve fibers are composed of axons, fibroblasts (Fbs), and Schwann cells (SCs), as well as macrophages, neutrophils, and vascular endothelial cells. Fbs within the nerve compartment provide an environment conductive to neuronal regeneration (Dreesmann et al., 2009). Following peripheral nerve transection, ephrin-B/EphB2-mediated cell sorting of Fbs and SCs is followed by directional SC migration into the transection site. These SCs then guide regrowing axons across the site to bridge the transection (Parrinello et al., 2010; Cattin et al., 2015; Dun et al., 2019). Fbs release neuregulin-1β1, a soluble pro-migratory factor, to promote SC migration (Dreesmann et al., 2009). Epineurial Fb-conditional medium (CM) enhances SC migration and neurite outgrowth of sensory neurons (van Neerven et al., 2013). SC migration is accelerated by tenascin-C, which is secreted by Fbs and exerts its effects through the integrin β1 signaling pathway (Zhang et al., 2016). Co-transplantation of Fbs with SCs enhances peripheral nerve regeneration and functional recovery (Wang et al., 2017). The effects of Fbs on peripheral nerve regeneration may result from modulation of SC proliferation and migration and enhancement of neurite sprouting and directional growth.

In a previous study, we found that Fbs in peripheral motor nerves express different genes from those in sensory nerves (He et al., 2018). This study aimed to investigate the effects of nerve Fbs (N-Fbs) on neurite outgrowth of motoneurons and to elucidate the underlying mechanisms.

Key Laboratory of Neuroregeneration of Jiangsu and Ministry of Education, Co-Innovation Center of Neuroregeneration, Jiangsu Clinical Medicine Center of Tissue Engineering and Nerve Injury Repair, Nantong University, Nantong, Jiangsu Province, China

*Correspondence to: Fei Ding, MS, dingfei@ntu.edu.cn.

https://orcid.org/0000-0002-7924-7545 (Qian-Ru He); https://orcid.org/0000-0002-9517-2707 (Fei Ding)

#Both authors contributed equally to this study.

Funding: *This study was supported by the National Key Research and Development Program of China, No. 2017YFA0104703 (to FD); the National Natural Science Foundation of China (Major Program), No. 92068112 (to FD); Science and Technology Program of Nantong of China, No. JC2020035 (to QRH); National Natural Science Foundation of China, Nos. 31500927 (to QRH) and 31870977 (to HYS) and the Priority Academic Program Development of Jiangsu High Education Institutions (PAPD) (to FD).*

How to cite this article: *He QR, Cong M, Yu FH, Ji YH, Yu S, Shi HY, Ding F (2022) Peripheral nerve fibroblasts secrete neurotrophic factors to promote axon growth of motoneurons. Neural Regen Res 17(8):1833-1840.*

Materials and Methods

Animals

All animals were provided by the Experimental Animal Center of Nantong University, China (animal license No. SCXK (Su) 2008-0010). All animal procedures were carried out in accordance with the Institutional Animal Care Guidelines of Nantong University and approved by the Jiangsu Provincial Administration Committee of Experimental Animals (approval No. 20150305-030).

Nerve fibroblast, cardiac fibroblast, and motoneurons culture and treatments

Cardiac fibroblast (C-Fbs) were selected to prove that fibroblasts from different tissues secrete different factors to regulate different functions. Compared with N-Fbs, C-Fbs come from different germinal layer and are easier to obtain and culture. N-Fbs were obtained from 1-day old Sprague-Dawley rats (*n* = 24) as described previously (He et al., 2012, 2020). Briefly, the animals were anesthetized with 5% isoflurane (RWD Life Technology Co., Ltd., Shenzhen, Guangdong Province, China) administered at a flow rate of 4 L/min for 2–3 minutes and sacrificed by decapitation. They were then sanitized using 70% ethanol before harvesting both sciatic nerves. The nerves were sliced into 3 mm-thick pieces using microscissors and the pieces were sequentially digested with collagenase (3 mg/mL; Thermo Fisher Scientific, Inc., Waltham, MA, USA) for 30 minutes and 0.125% (w/v) trypsin (Thermo Fisher Scientific, Inc.) for 10 minutes. The cells were cultured in DMEM containing 10% fetal bovine serum and 1% penicillin/streptomycin (Thermo Fisher Scientific, Inc.) at 37°C in the presence of 5% CO_2 for 4–5 days. The cell preparation was subjected to sequential differential digestion and adhesion to remove SCs and harvest N-Fbs. N-Fbs were identified by immunocytochemical staining for the fibroblast marker CD90 (Sorrell and Caplan, 2009).

After removing both sciatic nerves, the hearts were harvested to obtain C-Fbs as described previously (Thum et al., 2008). Briefly, after harvesting, the hearts were washed with D-Hank's solution (Thermo Fisher Scientific, Inc.) and sliced into 1–2 mm pieces. The pieces were digested with 0.125% (w/v) trypsin for 30 minutes at 37°C. The collected cell pellets were filtered through a 400 mesh filter and seeded onto uncoated culture dishes for incubation at 37°C for 60 minutes. The supernatant (containing the cardiomyocytes) was discarded and adherent cells were cultured in DMEM containing 10% fetal bovine serum and 1% penicillin/streptomycin at 37°C in the presence of 5% CO_2 for 4–5 days. The cell preparation was passaged until reaching 90% confluency, followed by differential adhesion for harvesting C-Fbs. C-Fbs were identified by CD90 immunocytochemical staining.

Primary motoneuron cultures were prepared as previously described (Haastert et al., 2005). Pregnant rats at 13.5–14 days of gestation were anesthetized with 5% isoflurane for 2–3 minutes and sacrificed by cervical dislocation. The fetuses were removed and placed in ice-cold Leibovitz's L-15 medium (Thermo Fisher Scientific, Inc.). The spinal cords were harvested and sliced into 1–2 mm pieces, which were then digested in 0.125% trypsin for 30 minutes. The cell suspension was purified using 15% OptiPrep gradient centrifugation solution (MilliporeSigma, St. Louis, MO, USA). The density-separated motoneurons were seeded on poly-L-lysine precoated culture plates (MilliporeSigma) and cultured with Neurobasal medium containing 2% B27 and 1% glutamax (Thermo Fisher Scientific, Inc.). Motoneurons were identified by immunocytochemical staining for the motoneuron marker choline acetyltransferase (ChAT) (Rodríguez-Cueto et al., 2021).

To detect phosphorylated tyrosine kinase B (p-TrkB), after motoneurons were cultured for 24 hours, Neurobasal medium was replaced with N-Fbs-CM, and immunocytochemical staining or western blotting was performed after culturing for 5, 15 and 30 minutes. The control group was replaced with Neurobasal medium (*n* = 30–40 fetal rats). To detect phosphorylated extracellular regulated protein kinase (p-ERK) and phosphorylated serine/threonine kinase (p-AKT), after motoneurons were cultured for 24 hours, Neurobasal medium was replaced with N-Fbs-CM, and western blotting was performed after culturing for 5, 15, and 30 minutes. The control group was replaced with Neurobasal medium (*n* = 30–40 fetal rats). To detect the effect of U0126 (a potent ERK inhibitor) and MK2206 (potent AKT inhibitor), after motoneurons were cultured for 24 hours, Neurobasal medium was replaced with U0126 (10 μM), MK2206 (0.5 and 2 μM), or ANA-12 (10 μM; a TrkB receptor antagonist (Arbat-Plana et al., 2017) and cultured for 1 hour. Then, the medium was replaced with N-Fbs-CM and western blotting was performed after culturing for 15 minutes. The control group was replaced with Neurobasal medium (*n* = 30–40 fetal rats).

Immunocytochemical staining

A preparation of N-Fbs, C-Fbs, or motoneurons was fixed using 4% paraformaldehyde (pH 7.4) for 15–20 minutes at room temperature. The cell samples were blocked with blocking buffer (0.01 M phosphate buffered saline containing 0.1% Triton X-100 and 10% goat serum) at 37°C for 30–45 minutes, and then incubated respectively with the following primary antibodies at 4°C overnight: mouse anti-CD90 antibody (Abcam, Cambridge, MA, USA, Cat# ab225, RRID: AB_2203300, 1:400), mouse anti-β-tubulin Ш antibody (Abcam, Cat# ab7751, RRID:AB_306045, 1:400), rabbit anti-neurofilament 200 (NF200) antibody (MilliporeSigma, Cat# N4142, RRID: AB_477272, 1:400), rabbit anti-brain-derived neurotrophic factor (BDNF) antibody (Abcam, Cat# ab226843, RRID: AB_2889875, 1:500), phalloidin from Amanita phalloides and phalloidin conjugates (MilliporeSigma, Cat# P2141, 1:800), rabbit anti-p-TrkB (MilliporeSigma, Cat# ABN1381, RRID: AB_2721199, 1:500), mouse anti-F-actin antibody (Abcam, Cat# ab130935, 1:400), mouse anti-β-Actin antibody (Abcam, Cat# ab8224, RRID: AB_449644, 1:400), and rabbit anti-ChAT antibody (Abcam, Cat# ab181023, RRID: AB_2687983, 1:200). Then, the samples were correspondingly incubated with secondary antibodies at room temperature in the dark for 2 hours: goat anti-rabbit IgG H&L Cy3 (Abcam, Cat# ab6939, RRID: AB_955021, 1:500), goat anti-mouse IgG Alexa Fluor 594 (Thermo Fisher Scientific, Inc., Cat# A-21125, RRID: AB_2535767, 1:500), and goat anti-mouse IgG H&L Alexa Fluor 488 (Abcam, Cat# ab150113, RRID: AB_2576208, 1:500). The samples were also counterstained with 5 mg/mL Hoechst 33342 (Abcam, Cat# ab228551) for 10 minutes. Images were captured using a confocal laser scanning microscope (TCS SP5; Leica Microsystems, Wetzlar, Germany).

To determine the effect of N-Fbs on neurite outgrowth of motoneurons, β-tubulin III immunostaining was performed following different treatments. Then, average neurite length and average number of neurite branches were assessed for approximately 300 motoneurons (*n* = 30–40 fetal rats for each time point) using ImageJ software (version 1.8.0; National Institutes of Health, Bethesda, MD, USA).

To determine BDNF expression in N-Fbs and C-Fbs, BDNF immunostaining was performed before 15 fields (*n* = 24 neonatal rats) were randomly selected and semi-quantitatively analyzed using ImageJ software. Mean fluorescence intensity (mean density) was calculated.

To determine the effect of N-Fbs on growth cone morphology of motoneurons, rhodamine-conjugated phalloidin (marked F-actin) staining was performed to visualize approximately 80–100 growth cones.

To determine the expression of F-actin and β-actin in motoneurons, staining with rhodamine-conjugated phalloidin and β-actin was performed before the 15 fields were randomly selected. The images were semi-quantitatively analyzed using ImageJ software. Mean fluorescence intensity (mean density) was calculated (*n* = 30–40 fetal rats).

Co-culture of motoneurons with N-Fbs or C-Fbs

Transwell co-culture, Fbs and motoneurons co-culture were used to verify the effect of N-Fbs on motoneuron neurite outgrowth.

Transwell co-culture

Co-culture of motoneurons with N-Fbs or C-Fbs was conducted in a 6.5 mm Transwell plate with 8 mm pores (Corning, Inc., Corning, NY, USA). Briefly, motoneurons (4×10^4/well) were inoculated onto poly-L-lysine-coated slides at the bottom of a Transwell plate with the Neurobasal medium containing 2% B27 and 1% glutamax being changed after 4 hours of culture. Then, N-Fbs or C-Fbs (4×10^4/well) in serum-free DMEM were seeded onto the upper chamber of the Transwell plate. Motoneurons were cultured in blank solution to serve as control. After co-culture for 12 or 24 hours, motoneurons were immunostained with anti-β-tubulin Ш to analyze neurite length and branch number (*n* = 30–40 fetal rats; *n* = 24 neonatal rats for each time point). To study the effects of ANA-12 treatment on neurite outgrowth, motoneurons were divided into three groups: blank, N-Fbs co-culture, and N-Fbs co-culture plus ANA-12 (10 μM). After co-culture for 24 hours, motoneurons were immunostained with anti-β-tubulin Ш to analyze neurite length and branch number (*n* = 30–40 fetal rats; *n* = 24 neonatal rats). To detect the inhibition of

β-actin and F-actin expression by U0126 and MK2206, motoneurons were divided into five groups: blank, N-Fbs co-culture, N-Fbs co-culture plus U0126 (10 μM), N-Fbs co-culture plus MK2206 (2 μM), and N-Fbs co-culture plus U0126 (10 μM) and MK2206 (2 μM). After motoneurons were cultured for 1 hour, the medium was replaced with Neurobasal medium and cultured for 24 or 48 hours. Then, immunocytochemistry and western blotting were performed to detect β-actin and F-actin expression (*n* = 30–40 fetal rats for each time point).

Fbs and motoneurons co-culture

N-Fbs or C-Fbs (2×10^4/well) were inoculated onto slides with DMEM containing 10% fetal bovine serum and 1% penicillin/streptomycin. After culture for 24 hours, motoneurons (4×10^4/well) were seeded onto the slides with Neurobasal medium containing 2% B27 and 1% glutamax being changed after 4 hours of culture. Motoneurons were cultured in blank solution to serve as control. After co-culture for 12 or 24 hours, cells were immunostained with CD90 (marked Fbs) and NF200 (marked motoneurons) to analyze neurite length and branch number (*n* = 30–40 fetal rats; *n* = 24 neonatal rats for each time point).

Preparation of conditional medium

The purified N-Fbs or C-Fbs were seeded onto 24-well plates at a density of 1×10^5/well for 24 hours of culturing (*n* = 24 neonatal rats). Then, the medium was replaced with Neurobasal medium containing 2% B27 and 1% glutamax and cultured for 36 hours. The supernatant was collected as N-Fbs-CM or C-Fbs-CM, which were filtered with a 0.22 μm filter for subsequent experiments.

Enzyme-linked immunosorbent assay (ELISA) was performed on the collected N-Fbs-CM or C-Fbs-CM to detect the BDNF level using a rat BDNF ELISA kit (CUSABIO, Cat# CSB-E04504r, Huamei Bioengineering Co., Ltd., Wuhan, China) in accordance with manufacturer instructions (*n* = 30–40 fetal rats).

Neurite outgrowth of motoneurons in microfluidic devices

To evaluate the *in vitro* effect of Fbs CM on neurite outgrowth of motoneurons, microfluidic devices with 150 μm microgrooves (SND 150, Xona Microfluidics, Temecula, CA, USA) were assembled as described previously (Taylor et al., 2005; Park et al., 2006). These devices can be used to compartmentalize neuronal neurites and somas. Briefly, after sterilization under ultraviolet irradiation, the microfluidic device was attached to the poly-L-lysine precoated culture dish. Motoneurons were then resuspended using Neurobasal medium containing 2% B27 and 1% glutamax and 10 μL of cell suspension (2×10^7/mL) was loaded into the soma chamber of the microfluidic device for 3 days of culture. Subsequently, the medium was replaced by N-Fbs-CM or C-Fbs-CM and cultured for 12 or 24 hours before β-tubulin III immunostaining. Images were taken using an inverted fluorescence microscope (DMi8, Leica). Average length was assessed for the 15 longest neurites (*n* = 30–40 fetal rats; *n* = 24 neonatal rats for each time point).

mRNA sequencing

Total RNA of N-Fbs or C-Fbs was extracted using TRIzol reagent (Invitrogen, Corp., Carlsbad, CA, USA), quality-checked using the Agilent 2100 Bioanalyzer (Agilent Technologies, Palo Alto, CA, USA) and NanoDrop spectrophotometer (Thermo Fisher Scientific, Inc.), and quantified by electrophoresis on a 1% agarose gel. RNA samples (1 μg) with a RNA integrity number value above 6.5 were used for the following library preparation. Sequences were processed and analyzed by GeneWiz (South Plainfield, NJ, USA). The library preparation was constructed according to manufacturer protocol. Next, libraries with different indices were multiplexed and loaded onto an Illumina HiSeq instrument (Illumina, San Diego, CA, USA). The sequencing was performed using a 2 × 150 base pair paired-end configuration. Image analysis and base calling were conducted using the HiSeq control software (HCS) + OLB + GAPipeline-1.6 on the HiSeq instrument (*n* = 24 neonatal rats). The raw mRNA sequencing data are shown in **Additional Table 1**.

Differential expression analysis and functional categorization

The differential expression analysis was carried out using the DESeq2 Bioconductor package (http://bioconductor.org/). To detect differentially expressed genes, estimates of dispersion and logarithmic fold changes were incorporated into the data-driven prior distributions and the adjusted *P* values of genes were set to < 0.05. To clarify the biological significance of differently expressed genes, the genes were categorized as biological process (BP), molecular function (MF), or cellular component (CC) using the Gene Ontology Seq R package (v1.34.1) (http://geneontology.org/) (Young et al., 2010).

Quantitative real-time polymerase chain reaction

To verify the nine differentially expressed genes obtained by mRNA sequencing, TRIzol reagent was used to extract the total RNA of N-Fbs and C-Fbs. Omniscript RT Kit (Qiagen, Valencia, CA, USA) was used to synthesize cDNA according to specifications. FastStart SYBR green quantitative real-time polymerase chain reaction (qPCR) Master Mix was used to perform qPCR with the CFX96 Real-Time PCR System (Bio-Rad, Singapore). The reaction mixture consisted of 10 μL SYBR Green qPCR Master Mix (Roche, Mannheim, Germany), 2 μL cDNA from each sample, 1 μL of each primer, and 6 μL RNase/DNase-free water. After amplification, the melting curves were analyzed. The qPCR products were quantified using the $2^{-\Delta\Delta CT}$ method (Bubner and Baldwin, 2004). The primers (**Additional Table 2**) used in the qPCR were provided by Generay Biotech Co. Ltd. (Shanghai, China) (*n* = 24 neonatal rats).

Western blot analysis

In order to observe the changes of corresponding protein expression, the M-PER mammalian protein extraction reagent (Pierce, Rockford, IL, USA) was used to extract the protein samples from N-Fbs, C-Fbs, or motoneurons. The protein samples were quantified using the bicinchoninic acid protein assay kit (Pierce). After electrophoresis was performed on 10 μg of total protein on a 10% or 12% (w/v) sodium dodecyl sulfate polyacrylamide gel, the protein was transferred onto a polyvinylidene fluoride membrane (MilliporeSigma). The membrane was incubated at 4°C overnight with the following primary antibodies: rabbit anti-BDNF antibody (1:1000), rabbit anti-p-TrkB antibody (1:500), mouse anti-F-actin (1:500), rabbit anti-Akt antibody (Cell Signaling Technology, Beverly, MA, USA, Cat# 9272, RRID: AB_329827, 1:1000), rabbit anti-phospho-Akt (Ser473) antibody (Cell Signaling Technology, Cat# 4060, RRID: AB_2315049, 1:2000), rabbit anti-p44/42 MAPK (Erk1/2) antibody (Cell Signaling Technology, Cat# 9102, RRID: AB_330744, 1:1000), rabbit anti-phospho-p44/42 MAPK (Erk1/2) (Thr202/Tyr204) antibody (Cell Signaling Technology, Cat# 4377, RRID:AB_331775, 1:1000), and rabbit anti-ATPase antibody (Abcam, Cat# ab76020, RRID: AB_1310695, 1:10,000). Then, the membranes were correspondingly incubated with secondary antibodies for 1 hour at room temperature: HRP-labeled goat anti-mouse IgG (Abcam, Cat# ab205719, RRID: AB_2755049, 1:5000) and HRP-labeled goat anti-rabbit IgG (Abcam, Cat# ab205718, RRID: AB_2819160, 1:5000). The enhanced chemiluminescence reagent kit (Beyotime, Shanghai, China) was used to detect the positive signals of membranes. Immunoreactive band intensity was analyzed using ImageJ software. GAPDH, β-actin, and ATPase were used as the internal reference. The original uncropped western blot images are shown in **Additional Figure 1**.

Immunohistochemistry

To avoid the interference of estrogen, male rats were selected to observe the expression of BDNF after sciatic nerve transection. Adult male Sprague-Dawley rats weighing 180 g were anesthetized using intraperitoneal sodium pentobarbital (30 mg/kg) before transection of the right sciatic nerve. The animals were divided into three groups (four rats per group): control, 3-day transection, and 7-day transection. At 3 or 7 days after nerve transection, rats were deeply anesthetized and perfused sequentially with normal saline (150 mL) and 4% paraformaldehyde (300 mL). The sciatic nerve was removed, postfixed at 4°C overnight, and dehydrated in a series of graded sucrose solutions. Then, the nerve was embedded by optimal cutting temperature compound, frozen in freezing microtome and cut into serial transverse sections at 12 μm intervals.

The nerve sections were blocked with blocking buffer (0.01 M PBS containing 0.1% Triton X-100 and 10% goat serum) at 37°C for 30–45 minutes followed by incubation with primary antibodies at 4°C in a humidified chamber overnight: mouse anti-CD90 antibody (1:400) or rabbit anti-BDNF antibody (1:500). After washing with PBS, the sections were correspondingly incubated with secondary antibodies for 2 hours in dark at room temperature: goat anti-rabbit IgG H&L Cy3 (1:500) or goat anti-mouse IgG H&L Alexa Fluor 488 (1:500). Finally, the samples were stained with 5 mg/mL Hoechst 33342 for 10 minutes at room temperature. Images were captured using a confocal laser scanning microscope.

Statistical analysis
Sample sizes were not predetermined using statistical methods; however, our sample sizes are similar to those reported in a previous publication (Yu et al., 2021). No animals or data points were excluded from the analysis. The evaluator was blinded to grouping. All data were normally distributed. Data are expressed as means ± standard error of the mean. Means were compared using the unpaired Student's *t*-test (two-tailed), one-way analysis of variance (followed by Tukey's *post hoc* test), or two-way analysis of variance (followed by Tukey's *post hoc* test) as appropriate. Statistical analyses were performed using Prism 6.0 software (GraphPad Software, San Diego, CA, USA). $P < 0.05$ was considered significant.

Results

Effect of N-Fbs on neurite outgrowth of motoneurons *in vitro*
The cell morphology of N-Fbs, C-Fbs, and motoneurons from primary culture was viewed under a phase-contrast microscope (**Additional Figure 2A–C**). Fbs were identified by the marker CD90 and motoneurons by ChAT and β-tubulin Ш (**Additional Figure 2D–G**). Cell nuclei were identified by Hoechst 33342 staining (**Additional Figure 2H** and **I**). N-Fb, C-Fb, and motoneuron cell purity was 93%, 88%, and 96%, respectively (**Additional Figure 2M**). These N-Fbs, C-Fbs, and motoneurons were used in subsequent experiments.

The Transwell co-culture experiments were carried out to investigate the effect of Fbs from two different tissues on motoneuron neurite outgrowth. Following co-culture with motoneurons for 12 hours, N-Fbs showed a trend of promoting neurite outgrowth but without statistical difference compared to C-Fbs ($P = 0.4246$). Following co-culture for 24 hours, N-Fbs significantly enhanced neurite growth ($P = 0.0025$) but failed to affect neurite branch number ($P = 0.6077$). C-Fbs co-cultured with motoneurons failed to promote neurite outgrowth ($P = 0.8533$; **Figure 1**). The results from culture of motoneurons in N-Fbs-CM or C-Fbs-CM for 12 hours ($P = 0.1244$) and 24 hours ($P = 0.0012$) showed similar results as the Transwell co-culture experiments (**Figure 2A–C**). The results from co-culture of motoneurons with N-Fbs or C-Fbs for 12 hours ($P = 0.0064$) and 24 hours ($P = 0.0018$) indicated that N-Fbs significantly augmented neurite length compared with C-Fbs and the neurites grew along the N-Fbs (**Figure 2D–H**).

mRNA sequencing analysis of N-Fbs and C-Fbs
mRNA sequencing identified 491 genes that were expressed differentially in N-Fbs and C-Fbs (**Figure 3A** and **B** and **Additional Table 3**). Among these, 130 were significantly upregulated in N-Fbs compared with C-Fbs (**Additional Table 4**), and 361 were significantly upregulated in C-Fbs compared with N-Fbs (**Additional Table 5**). To clarify the biological significance of the genes highly enriched in N-Fbs, Gene Ontology analysis was performed to categorize them according to biological function. The analysis demonstrated that they were involved in processes such as axon guidance, positive regulation of neuron projection, cartilage development, embryonic limb morphogenesis, positive regulation of transcription, and anterior/posterior pattern specification (**Figure 3C**).

qPCR validation of differentially expressed genes
Among all the differentially expressed genes, nine (*Ngfr*, *Nectin1*, *Dlx5*, *Bdnf*, *Fez1*, *Reln*, *Epha3*, *Serpine2*, and *Wnt5a*) were selected for qPCR validation due to their involvement in axon guidance and positive regulation of neuron projection development. qPCR analysis provided further evidence that these nine genes exhibited higher expression in N-Fbs than in C-Fbs (**Figure 3D**).

BDNF levels in N-Fbs at the peripheral nerve injury site *in vivo*
In humans, expression of BDNF and NGF is higher in N-Fbs than in SCs (Weiss et al., 2016). Our mRNA sequencing and qPCR experimental data demonstrated for the first time that Bdnf is highly expressed in rat N-Fbs. To further analyze BDNF expression and localization following peripheral nerve injury, we performed immunohistochemistry analysis at 3 and 7 days after sciatic nerve transection in rats. A previous study reported that Fbs accumulate at the nerve injury site (Parrinello et al., 2010). We found accumulation of a large number of Fbs in the proximal and distal stumps of the injured sciatic nerve 3 days after nerve injury. Furthermore, BDNF expression in Fbs was higher in injured nerves than in normal nerves (**Figure 4A** and **B**). BDNF was also expressed in SCs in the proximal and distal stumps 3 days after nerve injury (**Additional Figure 3**). On day 7 after nerve injury, the proximal and distal stumps were connected by a nerve bridge, a large number of Fbs had accumulated along the bridge, and level of BDNF expression was high at the site (**Figure 4C**).

Localization and secretion of BDNF in N-Fbs and C-Fbs
Immunocytochemistry showed that BDNF was mainly located in the cytoplasm and its expression was significantly higher in N-Fbs than in C-Fbs ($P = 0.0283$; **Figure 5A**, and **B**). Western blot analysis provided results consistent with those of immunohistochemistry staining ($P = 0.0092$; **Figure 5C**). ELISA showed that the BDNF level in the supernatant released from N-Fbs-CM was significantly higher than that in the supernatant released from C-Fbs ($P = 0.0009$; **Figure 5D**).

TrkB receptor inhibition abolished the growth promotion effects of N-Fbs *in vitro*
BDNF signaling is elicited through two cell surface receptors: the high affinity ligand-specific tropomyosin receptor kinase B (TrkB), and the low affinity p75 neurotrophin receptor ($p75^{NTR}$) (McGregor and English, 2019). To determine whether BDNF was produced by N-Fbs through TrkB receptor signaling, motoneurons were treated with N-Fbs-CM (cultured in N-Fbs-CM). Immunostaining showed that p-TrkB expression was significantly higher after treatment with N-Fbs-CM for 5 minutes and reached peak level after 15 minutes of treatment ($P < 0.0001$; **Figure 6A** and **B**). Western blot analysis confirmed the immunostaining results ($P = 0.0010$; **Figure 6C** and **D**).

A Transwell co-culture assay was used to investigate the effect of ANA-12 (a TrkB antagonist) on motoneuron neurite outgrowth. Interestingly, co-culture of motoneurons with Fbs plus ANA-12 significantly decreased neurite length compared to co-culture of motoneurons with Fbs alone ($P < 0.0001$); however, neurite branch number was not affected ($P = 0.7389$; **Figure 6E–G**).

BDNF effects were mediated via the ERK and AKT pathways *in vitro*
TrkB receptors contribute to promoting neuronal survival and growth through activation of the Ras/ERK and PI3-K/AKT pathways (Garraway and Huie, 2016). Therefore, ERK and AKT were analyzed in motoneurons after treatment with N-Fbs-CM. Both ERK ($P = 0.0017$) and AKT ($P = 0.0275$) were activated by N-Fbs-CM (**Figure 7A–C**). Moreover, U0126 (a potent ERK inhibitor) plus ANA-12 blocked ERK activity ($P = 0.0039$; **Figure 7D** and **E**) and varying concentrations of MK2206 (a potent AKT inhibitor) plus ANA-12 blocked AKT activity ($P < 0.0001$; **Figure 7F** and **G**).

Neuronal neurites regenerate through the formation of growth cones, which requires coordination of the cytoskeletal proteins actin and tubulin for axon growth and guidance (Patodia and Raivich, 2012). To determine whether the effects of BDNF on motoneuron neurite outgrowth were mediated via regulation of the actin cytoskeleton, immunostaining for F-actin and β-actin was performed. After co-culture of motoneurons with N-Fbs for 24 or 48 hours, the expression of F-actin and β-actin in motoneurons was significantly higher. Moreover, this increase was inhibited by U0126 and MK2206 (**Figure 8A–E**, and **Additional Figure 4**). Western blot analysis confirmed the results of immunostaining (**Figure 8H–I**).

Growth cones exhibit different shapes and numbers of filopodia and are classified as type I (collapsed), type II (partially collapsed), and type III (fan-shaped) (Lopez-Verrilli et al., 2013). In our study, after co-culture of motoneurons with N-Fbs for 24 and 48 hours, the percentage of type III (fan-shaped) growth cones was significantly higher; moreover, this increase was inhibited by U0126 and MK2206 (**Figure 8F**, and **G**).

Discussion

Fbs exist in all tissues and can be divided into distinct subtypes based on their tissue source, such as epithelial Fbs, dermal Fbs, N-Fbs, C-Fbs, and myoFbs. These Fbs interact with other cells and tissues such as epithelial tissues, SCs, and vascular endothelial cells during embryonic development and throughout life (Sorrell and Caplan, 2009; Bautista-Hernández et al., 2017; Davidson et al., 2021). In our study, N-Fbs significantly promoted motoneuron neurite outgrowth while C-Fbs had no significant effect. This suggests that Fbs from different tissue sources may secrete different factors and regulate different functions.

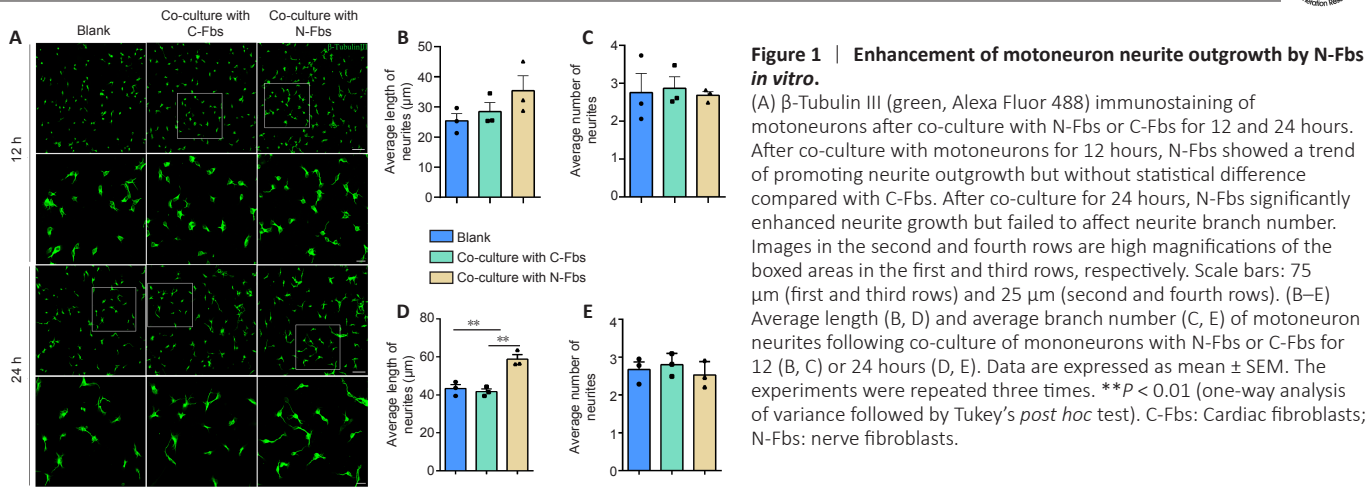

Figure 1 | Enhancement of motoneuron neurite outgrowth by N-Fbs *in vitro*.

(A) β-Tubulin III (green, Alexa Fluor 488) immunostaining of motoneurons after co-culture with N-Fbs or C-Fbs for 12 and 24 hours. After co-culture with motoneurons for 12 hours, N-Fbs showed a trend of promoting neurite outgrowth but without statistical difference compared with C-Fbs. After co-culture for 24 hours, N-Fbs significantly enhanced neurite growth but failed to affect neurite branch number. Images in the second and fourth rows are high magnifications of the boxed areas in the first and third rows, respectively. Scale bars: 75 μm (first and third rows) and 25 μm (second and fourth rows). (B–E) Average length (B, D) and average branch number (C, E) of motoneuron neurites following co-culture of mononeurons with N-Fbs or C-Fbs for 12 (B, C) or 24 hours (D, E). Data are expressed as mean ± SEM. The experiments were repeated three times. $^{**}P < 0.01$ (one-way analysis of variance followed by Tukey's *post hoc* test). C-Fbs: Cardiac fibroblasts; N-Fbs: nerve fibroblasts.

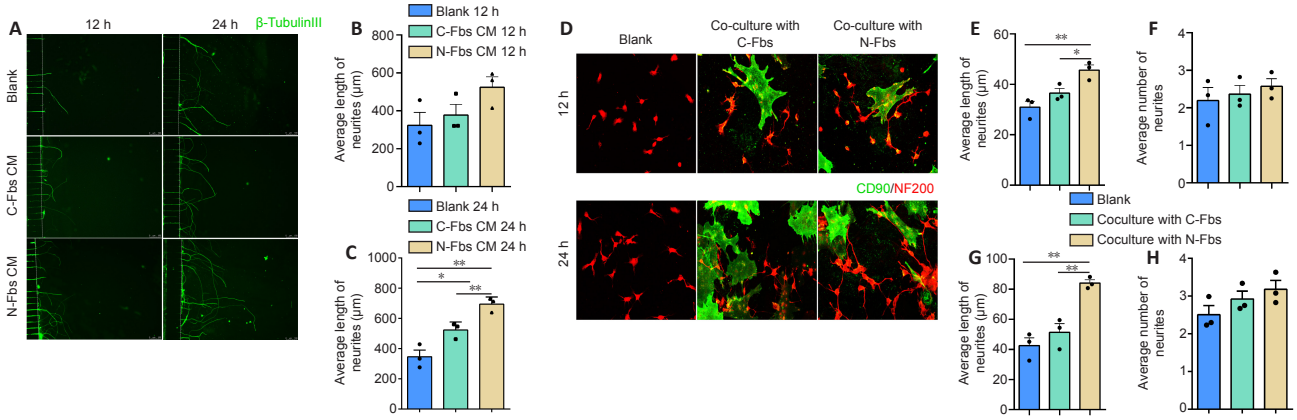

Figure 2 | Effects of N-Fbs or C-Fbs on neurite outgrowth of mononeurons *in vitro*.

(A) β-Tubulin III (green, Alexa Fluor 488) immunostaining of motoneurons after culture in N-Fbs-CM or C-Fbs-CM for 12 and 24 hours. Motoneurons cultured in N-Fbs-CM for 12 hours showed a trend toward growth promotion; significant growth promotion was seen after 24 hours. (B, C) Average motoneuron neurite length after culture in N-Fbs-CM or C-Fbs-CM for 12 hours (B) and 24 hours (C). (D) NF200 (red, Cy3) and CD90 (green, Alexa Fluor 488) immunostaining of motoneurons co-cultured with N-Fbs or C-Fbs for 12 and 24 hours. At 12 hours, N-Fbs increased neurite length compared with C-Fbs; the growth promoting effect was more obvious at 24 hours. Scale bars: 100 μm in A; 25 μm in D. (E–H) Average length (E, G) and average branch number (F, H) of motoneuron neurites following co-culture of motoneurons with N-Fbs or C-Fbs for 12 hours (E, F) and 24 hours (G, H). Data are expressed as mean ± SEM. The experiments were repeated three times. $^{*}P < 0.05$, $^{**}P < 0.01$ (one-way analysis of variance followed by Tukey's *post hoc* test). C-Fbs: Cardiac fibroblasts; C-Fbs-CM: cardiac fibroblasts conditioned medium; N-Fbs: nerve fibroblasts; N-Fbs-CM: nerve fibroblasts conditioned medium; NF200: neurofilament 200 .

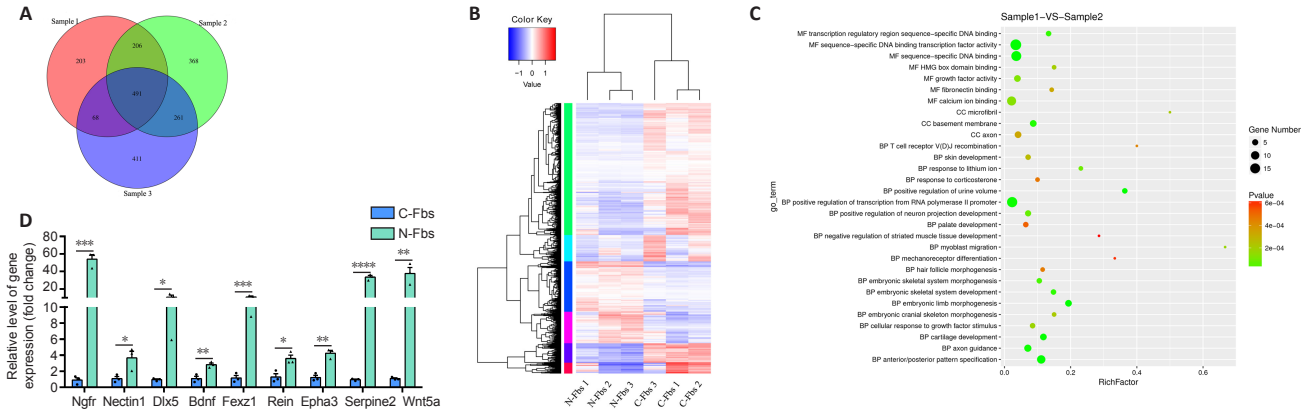

Figure 3 | mRNA sequencing analysis of N-Fbs and C-Fbs.

(A) Venn diagram depicting the genes identified by mRNA sequencing for three independent batches of biological samples, denoted as samples 1, 2, and 3. (B) Heatmap and cluster dendrogram of the 491 differentially expressed genes that showed more than two-fold changes in their expression. (C) Gene Ontology classification of 130 genes expressed highly in N-Fbs; the three categories are molecular function (MF), biological process (BP), and cellular component (CC). (D) qPCR data comparing the mRNA level of nine genes expressed differentially in N-Fbs and C-Fbs that are involved in axon guidance and positive regulation of neuron projection development. Gapdh served as an internal control. Data are expressed as mean ± SEM. The experiments were repeated three times. $^{*}P < 0.05$, $^{**}P < 0.01$, $^{***}P < 0.001$, $^{****}P < 0.0001$ (unpaired Student's *t*-test). Bdnf: Brain-derived neurotrophic factor; C-Fbs: cardiac fibroblasts; Dlx5: distal-less homeobox 5; Epha3: Eph receptor A3; Fez1: fasciculation and elongation protein zeta 1; Gapdh: glyceraldehyde 3-phosphate dehydrogenase; Nectin1: nectin cell adhesion molecule 1; N-Fbs: nerve fibroblasts; Ngfr: nerve growth factor receptor; qPCR: quantitative real-time polymerase chain reaction; Reln: reelin; Serpine2: serpin family E member 2; Wnt5a: wnt family member 5A.

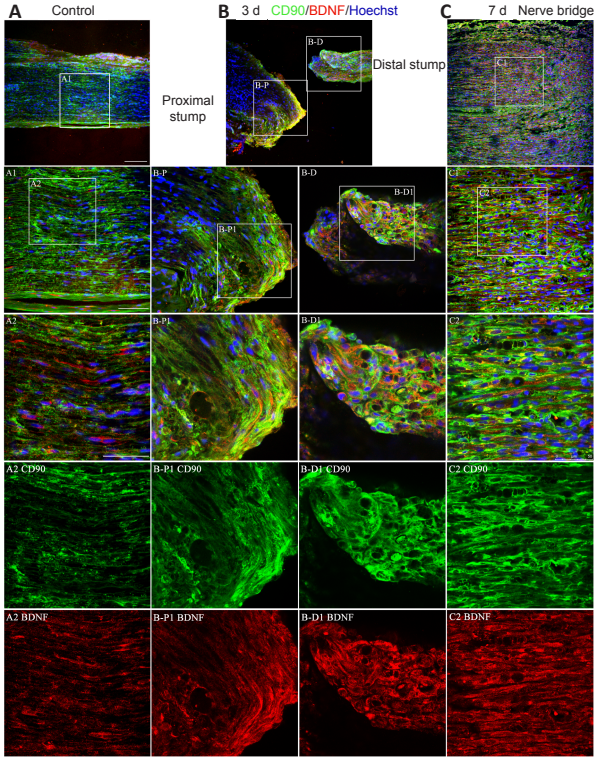

Figure 4 | BDNF expression in N-Fbs at injured and normal sciatic nerve sites in rats *in vivo*.

(A) BDNF expression in N-Fbs at the normal nerve site (control). (B) BDNF expression in N-Fbs at the injured nerve site 3 days after injury. (C) BDNF expression in N-Fbs at the bridge site 7 days after injury. Expression of BDNF was significantly higher in the proximal and distal stumps, and nerve bridge than in the control group 3 and 7 days after transection. Images in the top three lines are mergers of BDNF (red, Cy3), CD90 (green, Alexa Fluor 488), and Hoechst 33342 (blue) staining images. Images in the lower panels are high magnifications of the boxed areas in the upper panels. Scale bars: 50 μm. P and D indicate the proximal and distal stumps, respectively. BDNF: Brain-derived neurotrophic factor; N-Fbs: nerve fibroblasts.

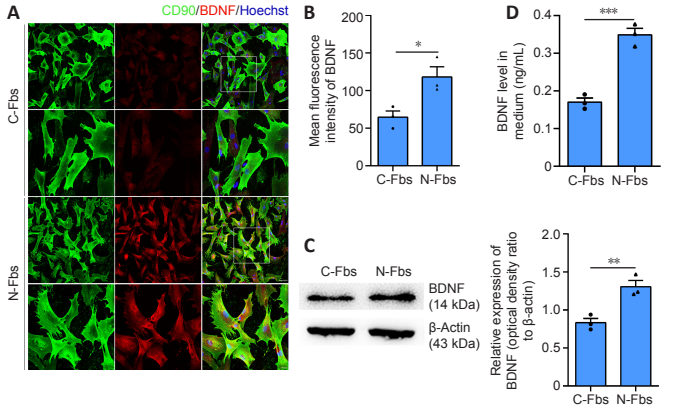

Figure 5 | BDNF expression in N-Fbs and C-Fbs.

(A) Immunocytochemistry showed that BDNF expression was significantly higher in primary cultured N-Fbs than in C-Fbs. BDNF (red, Cy3), CD90 (green, Alexa Fluor 488), and Hoechst 33342 (blue) staining, and their merged images for N-Fbs and C-Fbs are shown. Images in the lower panels are high magnifications of boxed areas in the upper panels. Scale bars: 75 μm (low-magnification), and 25 μm (high-magnification). (B) Mean fluorescence intensity of BDNF staining for N-Fbs and C-Fbs. (C) Representative western blot images (left) and the resulting histogram (right) comparing BDNF expression in N-Fbs and C-Fbs. (D) Enzyme-linked immunosorbent assay analysis comparing BDNF secretion from N-Fbs-CM and C-Fbs-CM. Data are expressed as mean ± SEM. The experiments were repeated three times. *P < 0.05, **P < 0.01, ***P < 0.001 (unpaired Student's t-test). BDNF: Brain-derived neurotrophic factor; C-Fbs: cardiac fibroblasts; C-Fbs-CM: cardiac fibroblasts conditioned medium; N-Fbs: nerve fibroblasts; N-Fbs-CM: nerve fibroblasts conditioned medium.

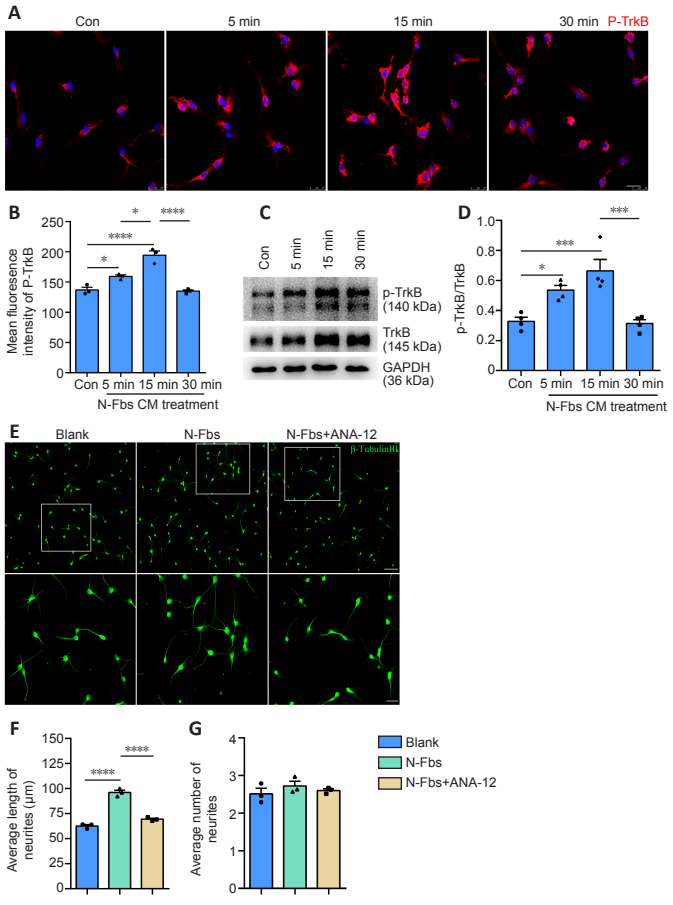

Figure 6 | N-Fbs effects are abolished by TrkB receptor inhibition.

(A) p-TrkB (red, Cy3) immunostaining of motoneurons after treatment with N-Fbs-CM for 0 (control, con), 5, 15, and 30 minutes. The expression of p-TrkB was significantly higher after treatment with N-Fbs-CM for 5 minutes and reached peak level after 15 minutes of treatment; after treatment for 30 minutes, expression returned to normal. Scale bar: 25 μm. (B) Mean immunofluorescence intensity of p-TrkB in motoneurons after treatment with N-Fbs-CM for 0 (control), 5, 15, and 30 minutes. (C) Representative images from western blot analysis of p-TrkB expression in motoneurons after treatment with N-Fbs-CM for 0 (control), 5, 15, and 30 minutes. (D) Quantitative western blot results (one-way analysis of variance followed by Tukey's *post hoc* test). (E) Immunostaining for β-tubulin Ш (green, Alexa Fluor 488) expression in motoneurons after co-culture with N-Fbs or N-Fbs plus ANA-12 for 24 hours. Co-culture of motoneurons with Fbs plus ANA-12 significantly decreased neurite length compared to co-culture of motoneurons with Fbs alone. Images in the lower panels are high magnifications of the boxed areas in the upper panels. Scale bar: 75 μm (low-magnification), and 25 μm (high-magnification). (F, G) Average length (F) and average branch number (G) of motoneuron neurites after co-culture with N-Fbs or N-Fbs plus ANA-12 for 24 hours. Data are expressed as means ± standard error of the mean. The experiments were repeated three times. *P < 0.05, ***P < 0.001, ****P < 0.0001 (one-way analysis of variance followed by Tukey's *post hoc* test). ANA-12: A TrkB receptor antagonist; N-Fbs: nerve fibroblasts; N-Fbs-CM: nerve fibroblasts conditioned medium; p-TrkB: phosphorylated tyrosine kinase B; TrkB: tyrosine kinase B.

Our unbiased mRNA sequencing revealed 491 genes that were expressed differentially between N-Fbs and C-Fbs. Among these, 130 genes involved in axon guidance, positive regulation of neuron projection, and positive regulation of transcription were significantly upregulated in N-Fbs compared with C-Fbs. Nine genes (*Ngfr*, *Nectin1*, *Dlx5*, *Bdnf*, *Fez1*, *Reln*, *Epha3*, *Serpine2*, and *Wnt5a*) involved in axon guidance and positive regulation of neuron projection development were confirmed by qPCR validation. Co-culture of motoneurons and N-Fbs in the same well, which simulates the *in vivo* environment, resulted in significantly increased neurite length and neurite growth along N-Fbs. The interaction of these axon guiding and projection proteins with their receptors on motoneurons may explain these findings.

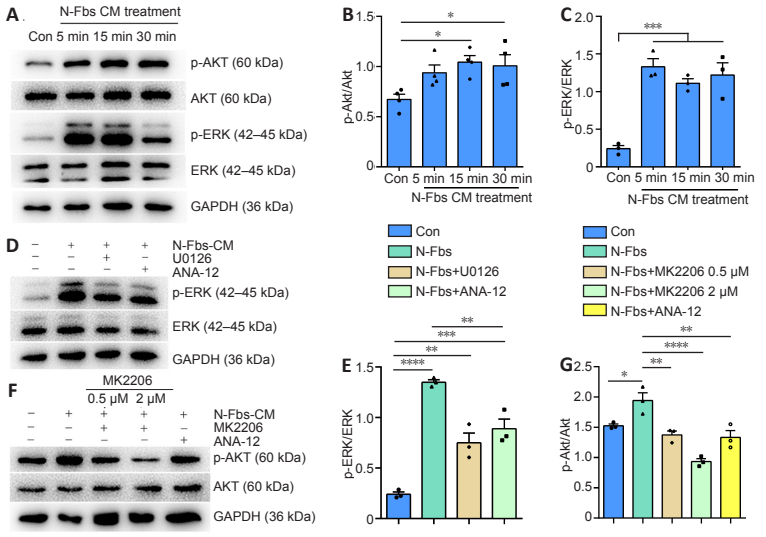

Figure 7 | Activation of ERK and AKT pathways by BDNF released from N-Fbs.

(A) Representative images of western blot analysis of p-AKT, AKT, p-ERK, and ERK expression in motoneurons after treatment with N-Fbs-CM for 0 (control, con), 5, 15, and 30 minutes. The expression of p-AKT was significantly higher after treatment with N-Fbs-CM for 5 minutes, reached peak level at 15 minutes of treatment, and was maintained at 30 minutes of treatment. The expression of p-ERK was significantly higher after treatment with N-Fbs-CM for 5 minutes, reached peak level at 5 minutes, and was maintained at 30 minutes of treatment. (B, C) Quantitative western blot analysis results from A. All tests were performed in quadruplicate (B) or triplicate (C). (D, E) Representative images of western blot analysis (D) and the resulting histogram (E) showing that p-ERK expression in motoneurons was inhibited by U0126 plus ANA-12. (F, G) Representative images of western blot analysis (F) and the resulting histogram (G) showing that p-AKT expression in motoneurons was inhibited by MK2206 plus ANA-12. Data are expressed as means ± standard error of the mean. The experiments were repeated four (B) or three (all others) times. $*P < 0.05$, $**P < 0.01$, $***P < 0.001$, $****P < 0.0001$ (one-way analysis of variance followed by Tukey's *post hoc* test). AKT: Serine/threonine kinase; ANA-12: a TrkB receptor antagonist; CM: conditional medium; ERK: extracellular regulated protein kinases; GAPDH: glyceraldehyde 3-phosphate dehydrogenase; MK2206: potent AKT inhibitor; N-Fbs: nerve fibroblasts; BDNF: brain-derived neurotrophic factor; N-Fbs-CM: nerve fibroblasts conditioned medium; p-AKT: phosphorylated serine/threonine kinase; p-ERK: phosphorylated extracellular regulated protein kinases; U0126: potent ERK inhibitor.

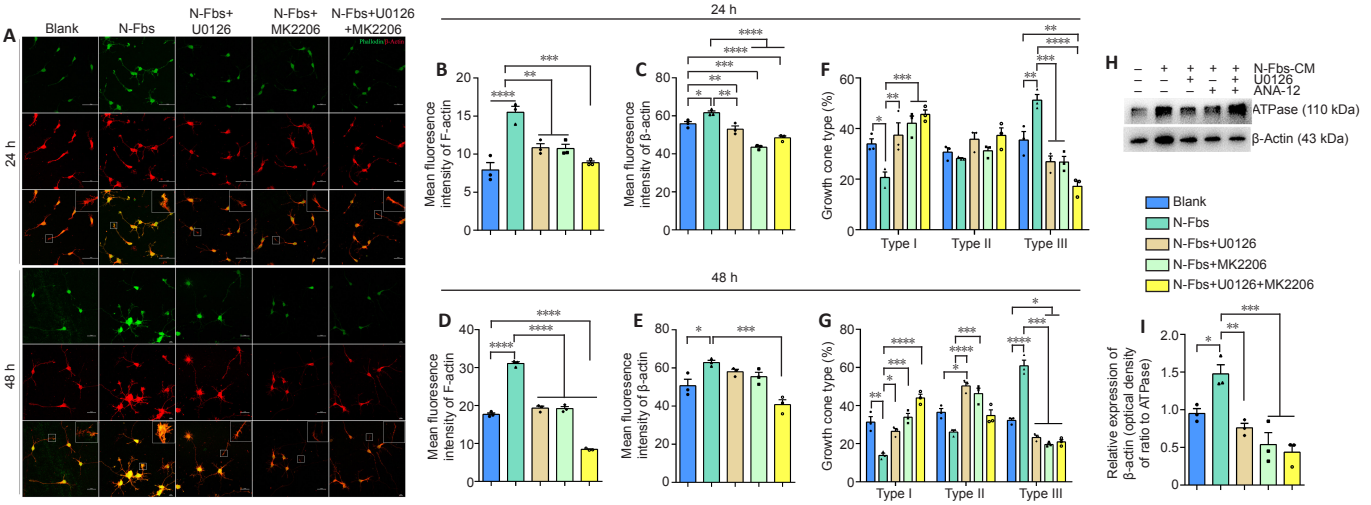

Figure 8 | F-actin and β-actin expression is increased by BDNF released from N-Fbs through the ERK and AKT pathways.

(A) Immunostaining showed that after co-culture of motoneurons with N-Fbs for 24 and 48 hours, the expression of F-actin (marked by phalloidin) and β-actin in motoneurons was significantly higher; this increase was inhibited by U0126 and MK2206. Phalloidin (green, Alexa Fluor 488) and β-actin (red, Cy3) immunostaining of motoneurons after co-culture with N-Fbs, N-Fbs + U0126, N-Fbs + MK2206, and N-Fbs + U0126 + MK2206 for 24 and 48 hours. The boxed area images show high magnifications of growth cones. Scale bar: 50 μm. (B–E) Mean fluorescence intensity of F-actin and β-actin in motoneurons after different treatments for 24 hours (B, C) and 48 hours (D, E). (F, G) Quantitative results of the percentage of different growth cone types in motoneuron neurites after different treatments for 24 hours (F) and 48 hours (G). (H, I) Representative images of western blot analysis (H) and the resulting histogram (I) for β-actin expression in motoneurons after different treatments for 48 hours. Data are expressed as means ± standard error of the mean. The experiments were repeated four (B) or three (all others) times. $*P < 0.05$, $**P < 0.01$, $***P < 0.001$, $****P < 0.0001$ (two-way analysis of variance followed by Tukey's *post hoc* test in F, G; one-way analysis of variance followed by Tukey's *post hoc* test in the others). AKT: Serine/threonine kinase; ATPase: adenosine triphosphatase; BDNF: brain-derived neurotrophic factor; ERK: extracellular regulated protein kinases; MK2206: potent AKT inhibitor; N-Fbs: nerve fibroblasts; U0126: potent ERK inhibitor.

BDNF is a member of the neurotrophin family and regulates neurogenesis, regeneration, and synaptic plasticity, as well as learning and memory (Richner et al., 2014; McGregor and English, 2019; Hernandez-Echeagaray, 2020; Turovskaya et al., 2020). In the peripheral nerve system, BDNF is synthesized and secreted by SCs, motoneurons, and a subset of dorsal root ganglia neurons (Wilhelm et al., 2012; Su et al., 2019). Moreover, the protein expression of BDNF or NGF is higher in human N-Fbs than in SCs (Weiss et al., 2016). However, the role of BDNF secreted by N-Fbs in the peripheral nervous system has not yet been fully elucidated.

BDNF is initially synthesized as a preproprotein and then cleaved into a mature protein (Seidah et al., 1996). Mature BDNF preferentially binds to the TrkB receptor, which results in pro-growth signaling, whereas proBDNF preferentially binds to the $p75^{NTR}$ receptor, which results in anti-growth signaling (Lee et al., 2001). In our study, western blot analysis suggested that the BDNF synthesized and secreted by N-Fbs is likely to be the mature BDNF (approximately 14 kDa), which binds to the TrkB receptor with high affinity and activates the Ras/ERK, PI3-K/AKT, and phospholipase C-γ pathways. The Ras/ERK and PI3-K/AKT pathways mediate neuron survival, growth, and plasticity while the phospholipase C-γ pathway activates protein kinase C to mediate neural plasticity (Chao, 2003; Garraway and Huie, 2016).

Immunostaining together with western blot analysis demonstrated that p-TrkB expression in motoneurons was significantly higher after treatment with N-Fbs-CM for 5 minutes and reached peak level after 15 minutes of treatment. ANA-12, an antagonist of TrkB, significantly inhibited neurite length of motoneurons following its addition to motoneurons co-cultured with N-Fbs; however, it had no significant effect on neurite branch number. These findings suggest that BDNF secreted from N-Fbs promotes neurite outgrowth in motoneurons through activation of TrkB receptor phosphorylation.

Similar to previous study (Garraway and Huie, 2016), our study also showed that BDNF secreted from N-Fbs resulted in activation of the ERK and AKT pathways in motoneurons. Blockade of both signaling pathways suggested that both were responsible for the promoting effect of BNDF on neurite growth.

Actin is a vital cytoskeletal protein with various isoforms including α-actin, β-actin, and γ-actin. β-Actin is highly abundant in growth cones of embryonic motoneurons and influences growth cone morphology. β-Actin knockdown reduces the dynamic movements of growth cone filopodia and results in smaller growth cones (Dombert et al., 2017; Moradi et al., 2017). BDNF treatment of mouse embryonic motoneurons reduces actin movement in growth cones because of a shift from globular β-actin (G-actin) to filamentous β-actin (F-actin) (Moradi et al., 2017). Our data indicate that BDNF secreted from N-Fbs affected motoneuron neurite outgrowth by promoting the expression of β-actin and F-actin through the ERK and AKT pathways.

During axon regeneration, growth cones project finger-like filopodia to guide neuron migration and neurite pathfinding (Hur et al., 2012; Marshall and Farah, 2021). In our study, treatment of motoneurons with N-Fbs-CM induced collapsed (type I) growth cones but increased the abundance of fan-shaped (type III) growth cones. These bi-directional effects were reversed by ERK and AKT pathway inhibitors, which may be attributed to the fact that fan-shaped (type III) growth cones with high motility are more helpful in neurite elongation (Goswami et al., 2007).

Taken together, we found that N-Fbs and C-Fbs exhibited different patterns of gene expression. N-Fbs, but not C-Fbs, significantly promoted neurite outgrowth of motoneurons *in vitro*. BDNF secreted from N-Fbs increased the expression of β-actin and F-actin through the ERK and AKT pathways and promoted motoneuron neurite outgrowth. Although our study has increased understanding of N-Fb function in motoneuron regrowth and provides a feasible strategy for peripheral nerve repair, it only focused on the role of BDNF secreted from N-Fbs. Future studies should investigate additional neurotrophic factors derived from N-Fbs.

Acknowledgments: *We thank Professor Jie Liu from Nantong University, China for assistance in manuscript preparation.*
Author contributions: *Study design: FD, QRH; study implementation: QRH, MC, FHY, HYS; data analysis and figure preparation: YHJ, SY; manuscript drafting: QRH, FD. All authors approved the final version of the manuscript.*
Conflicts of interest: *The authors declare no competing financial interest.*
Availability of data and materials: *The mRNA sequencing data are available via NCBI with biosample accession SAMN19221079/bioproject accession PRJNA730115.*

Open peer reviewers: *Xin-Peng Dun, Plymouth University, UK; Sarah D. Ackerman, University of Oregon, USA.*
Additional files:
Additional Figure 1: *Original uncropped Western blot images.*
Additional Figure 2: *Identification of N-Fbs, C-Fbs and motoneurons.*
Additional Figure 3: *BDNF positive expression in SCs at the injured or normal sciatic nerve site of rats.*
Additional Figure 4: *Lower-magnification image of Figure 8A.*
Additional Table 1: *The raw data of mRNA sequencing.*
Additional Table 2: *The primer sequences for quantitative real-time polymerase chain reaction.*
Additional Table 3: *List of 491 differentially expressed genes between N-Fbs and C-Fbs.*
Additional Table 4: *List of 130 higher expressed genes in N-Fbs than in C-Fbs.*
Additional Table 5: *List of 361 higher expressed genes in C-Fbs than in N-Fbs.*
Additional file 1: *Open peer review reports 1 and 2.*

References

Arbat-Plana A, Cobianchi S, Herrando-Grabulosa M, Navarro X, Udina E (2017) Endogenous modulation of TrkB signaling by treadmill exercise after peripheral nerve injury. Neuroscience 340:188-200.
Bautista-Hernández LA, Gómez-Olivares JL, Buentello-Volante B, Bautista-de Lucio VM (2017) Fibroblasts: the unknown sentinels eliciting immune responses against microorganisms. Eur J Microbiol Immunol (Bp) 7:151-157.
Bubner B, Baldwin IT (2004) Use of real-time PCR for determining copy number and zygosity in transgenic plants. Plant Cell Rep 23:263-271.
Cattin AL, Burden JJ, Van Emmenis L, Mackenzie FE, Hoving JJ, Garcia Calavia N, Guo Y, McLaughlin M, Rosenberg LH, Quereda V, Jamecna D, Napoli I, Parrinello S, Enver T, Ruhrberg C, Lloyd AC (2015) Macrophage-induced blood vessels guide schwann cell-mediated regeneration of peripheral nerves. Cell 162:1127-1139.
Chao MV (2003) Neurotrophins and their receptors: a convergence point for many signalling pathways. Nat Rev Neurosci 4:299-309.
Davidson S, Coles M, Thomas T, Kollias G, Ludewig B, Turley S, Brenner M, Buckley CD (2021) Fibroblasts as immune regulators in infection, inflammation and cancer. Nat Rev Immunol doi: 10.1038/s41577-021-00540-z.
Dombert B, Balk S, Lüningschrör P, Moradi M, Sivadasan R, Saal-Bauernschubert L, Jablonka S (2017) BDNF/trkB induction of calcium transients through Ca(v)2.2 calcium channels in motoneurons corresponds to F-actin assembly and growth cone formation on β2-chain laminin (221). Front Mol Neurosci 10:346.
Dreesmann L, Mittnacht U, Lietz M, Schlosshauer B (2009) Nerve fibroblast impact on Schwann cell behavior. Eur J Cell Biol 88:285-300.
Dun XP, Carr L, Woodley PK, Barry RW, Drake LK, Mindos T, Roberts SL, Lloyd AC, Parkinson DB (2019) Macrophage-derived Slit3 controls cell migration and axon pathfinding in the peripheral nerve bridge. Cell Rep 26:1458-1472.e4.
Garraway SM, Huie JR (2016) Spinal plasticity and behavior: BDNF-induced neuromodulation in uninjured and injured spinal cord. Neural Plast 2016:9857201.
Goswami C, Schmidt H, Hucho F (2007) TRPV1 at nerve endings regulates growth cone morphology and movement through cytoskeleton reorganization. FEBS J 274:760-772.
Haastert K, Grosskreutz J, Jaeckel M, Laderer C, Bufler J, Grothe C, Claus P (2005) Rat embryonic motoneurons in long-term co-culture with Schwann cells--a system to investigate motoneuron diseases on a cellular level in vitro. J Neurosci Methods 142:275-284.
He Q, Man L, Ji Y, Ding F (2012) Comparison in the biological characteristics between primary cultured sensory and motor Schwann cells. Neurosci Lett 521:57-61.
He Q, Yu F, Li Y, Sun J, Ding F (2020) Purification of fibroblasts and schwann cells from sensory and motor nerves in vitro. J Vis Exp:e60952.
He Q, Shen M, Tong F, Cong M, Zhang S, Gong Y, Ding F (2018) Differential gene expression in primary cultured sensory and motor nerve fibroblasts. Front Neurosci 12:1016.
Hernandez-Echeagaray E (2020) The role of the TrkB-T1 receptor in the neurotrophin-4/5 antagonism of brain-derived neurotrophic factor on corticostriatal synaptic transmission. Neural Regen Res 15:1973-1976.
Hur EM, Saijilafu, Zhou FQ (2012) Growing the growth cone: remodeling the cytoskeleton to promote axon regeneration. Trends Neurosci 35:164-174.
Lee R, Kermani P, Teng KK, Hempstead BL (2001) Regulation of cell survival by secreted proneurotrophins. Science 294:1945-1948.
Lopez-Verrilli MA, Picou F, Court FA (2013) Schwann cell-derived exosomes enhance axonal regeneration in the peripheral nervous system. Glia 61:1795-1806.
Marshall KL, Farah MH (2021) Axonal regeneration and sprouting as a potential therapeutic target for nervous system disorders. Neural Regen Res 16:1901-1910.
McGregor CE, English AW (2019) The role of BDNF in peripheral nerve regeneration: activity-dependent treatments and Val66Met. Front Cell Neurosci 12:522.
Moradi M, Sivadasan R, Saal L, Lüningschrör P, Dombert B, Rathod RJ, Dieterich DC, Blum R, Sendtner M (2017) Differential roles of α-, β-, and γ-actin in axon growth and collateral branch formation in motoneurons. J Cell Biol 216:793-814.
Park JW, Vahidi B, Taylor AM, Rhee SW, Jeon NL (2006) Microfluidic culture platform for neuroscience research. Nat Protoc 1:2128-2136.
Parrinello S, Napoli I, Ribeiro S, Wingfield Digby P, Fedorova M, Parkinson DB, Doddrell RD, Nakayama M, Adams RH, Lloyd AC (2010) EphB signaling directs peripheral nerve regeneration through Sox2-dependent Schwann cell sorting. Cell 143:145-155.
Patodia S, Raivich G (2012) Downstream effector molecules in successful peripheral nerve regeneration. Cell Tissue Res 349:15-26.
Richner M, Ulrichsen M, Elmegaard SL, Dieu R, Pallesen LT, Vaegter CB (2014) Peripheral nerve injury modulates neurotrophin signaling in the peripheral and central nervous system. Mol Neurobiol 50:945-970.
Rodríguez-Cueto C, Gómez-Almería M, García Toscano L, Romero J, Hillard CJ, de Lago E, Fernández-Ruiz J (2021) Inactivation of the CB(2) receptor accelerated the neuropathological deterioration in TDP-43 transgenic mice, a model of amyotrophic lateral sclerosis. Brain Pathol:e12972.
Seidah NG, Benjannet S, Pareek S, Chretien M, Murphy RA (1996) Cellular processing of the neurotrophin precursors of NT3 and BDNF by the mammalian proprotein convertases. FEBS Lett 379:247-250.
Sorrell JM, Caplan AI (2009) Fibroblasts-a diverse population at the center of it all. Int Rev Cell Mol Biol 276:161-214.
Su WF, Wu F, Jin ZH, Gu Y, Chen YT, Fei Y, Chen H, Wang YX, Xing LY, Zhao YY, Yuan Y, Tang X, Chen G (2019) Overexpression of P2X4 receptor in Schwann cells promotes motor and sensory functional recovery and remyelination via BDNF secretion after nerve injury. Glia 67:78-90.
Taylor AM, Blurton-Jones M, Rhee SW, Cribbs DH, Cotman CW, Jeon NL (2005) A microfluidic culture platform for CNS axonal injury, regeneration and transport. Nat Methods 2:599-605.
Thum T, Gross C, Fiedler J, Fischer T, Kissler S, Bussen M, Galuppo P, Just S, Rottbauer W, Frantz S, Castoldi M, Soutschek J, Koteliansky V, Rosenwald A, Basson MA, Licht JD, Pena JT, Rouhanifard SH, Muckenthaler MU, Tuschl T, et al. (2008) MicroRNA-21 contributes to myocardial disease by stimulating MAP kinase signalling in fibroblasts. Nature 456:980-984.
Turovskaya MV, Gaidin SG, Vedunova MV, Babaev AA, Turovsky EA (2020) BDNF overexpression enhances the preconditioning effect of brief episodes of hypoxia, promoting survival of GABAergic neurons. Neurosci Bull 36:733-760.
van Neerven SG, Pannaye P, Bozkurt A, Van Nieuwenhoven F, Joosten E, Hermans E, Taccola G, Deumens R (2013) Schwann cell migration and neurite outgrowth are influenced by media conditioned by epineurial fibroblasts. Neuroscience 252:144-153.
Wang Y, Li D, Wang G, Chen L, Chen J, Liu Z, Zhang Z, Shen H, Jin Y, Shen Z (2017) The effect of co-transplantation of nerve fibroblasts and Schwann cells on peripheral nerve repair. Int J Biol Sci 13:1507-1519.
Weiss T, Taschner-Mandl S, Bileck A, Slany A, Kromp F, Rifatbegovic F, Frech C, Windhager R, Kitzinger H, Tzou CH, Ambros PF, Gerner C, Ambros IM (2016) Proteomics and transcriptomics of peripheral nerve tissue and cells unravel new aspects of the human Schwann cell repair phenotype. Glia 64:2133-2153.
Wilhelm JC, Xu M, Cucoranu D, Chmielewski S, Holmes T, Lau KS, Bassell GJ, English AW (2012) Cooperative roles of BDNF expression in neurons and Schwann cells are modulated by exercise to facilitate nerve regeneration. J Neurosci 32:5002-5009.
Young MD, Wakefield MJ, Smyth GK, Oshlack A (2010) Gene ontology analysis for RNA-seq: accounting for selection bias. Genome Biol 11:R14.
Yu M, Gu G, Cong M, Du M, Wang W, Shen M, Zhang Q, Shi H, Gu X, Ding F (2021) Repair of peripheral nerve defects by nerve grafts incorporated with extracellular vesicles from skin-derived precursor Schwann cells. Acta Biomater 134:190-203.
Zhang Z, Yu B, Gu Y, Zhou S, Qian T, Wang Y, Ding G, Ding F, Gu X (2016) Fibroblast-derived tenascin-C promotes Schwann cell migration through beta1-integrin dependent pathway during peripheral nerve regeneration. Glia 64:374-385.

P-Reviewers: Dun XP, Ackerman SD; C-Editor: Zhao M; S-Editors: Yu J, Li CH; L-Editors: Yu J, Song LP; T-Editor: Jia Y

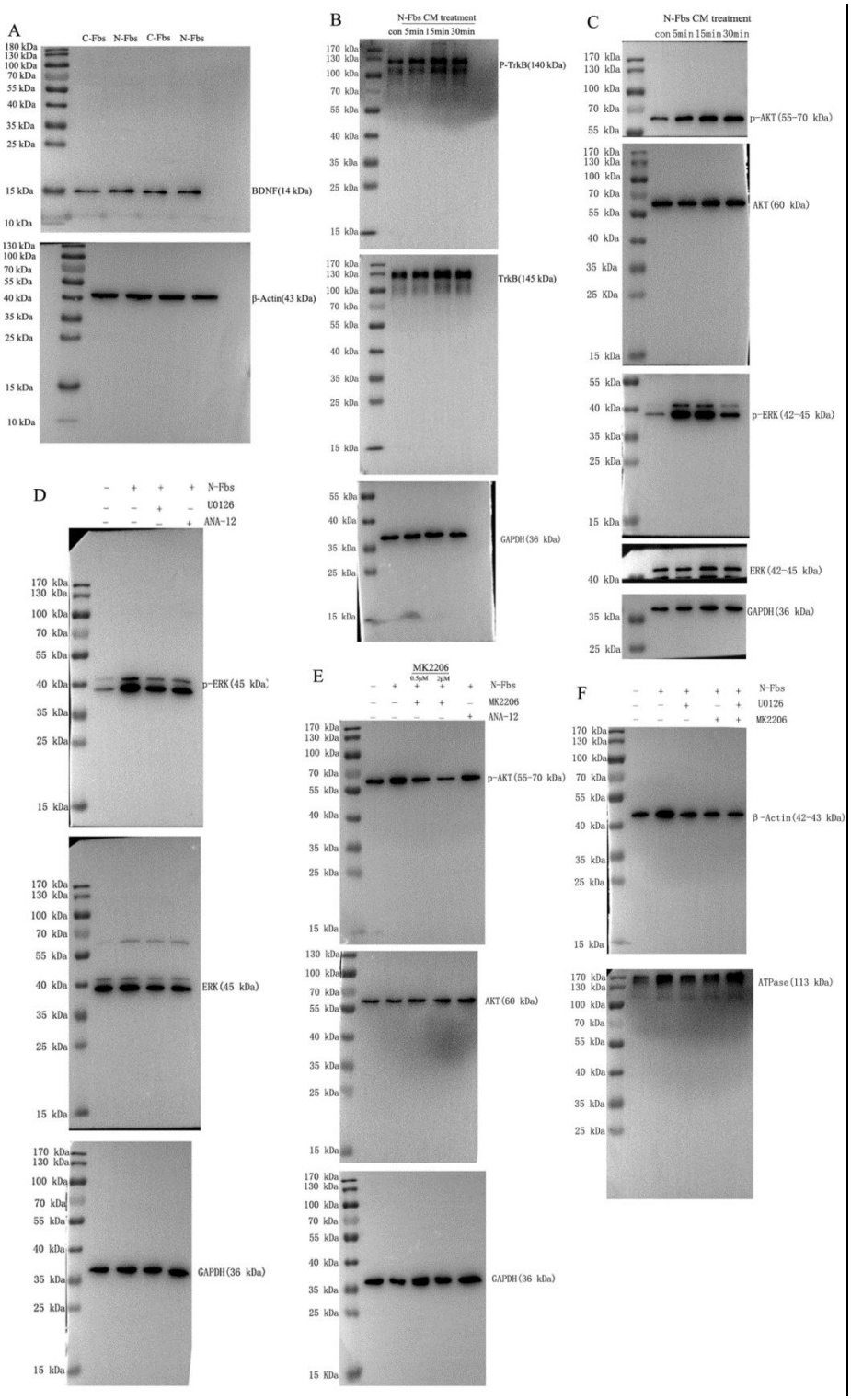

Additional Figure 1 Original uncropped Western blot images.

(A-F) Images were from which Figures 5C, 6C, 7A, D, E, and 8H. AKT: Serine/threonine kinase; ANA-12: a TrkB receptor antagonist; ATPase: Adenosine triphosphatase; BDNF: brain-derived neurotrophic factor; C-Fbs: cardiac fibroblasts; CM: conditional medium; ERK: extracellular regulated protein kinases; GAPDH: glyceraldehyde 3-phosphate dehydrogenase; MK2206: potent AKT inhibitor; N-Fbs: nerve fibroblasts; N-Fbs-CM: nerve fibroblasts conditioned medium; p-AKT: phosphorylated serine/threonine kinase; p-ERK: phosphorylated extracellular regulated protein kinases; p-TrkB: phosphorylated tyrosine kinase B; TrkB: tyrosine kinase B; U0126: potent ERK inhibitor.

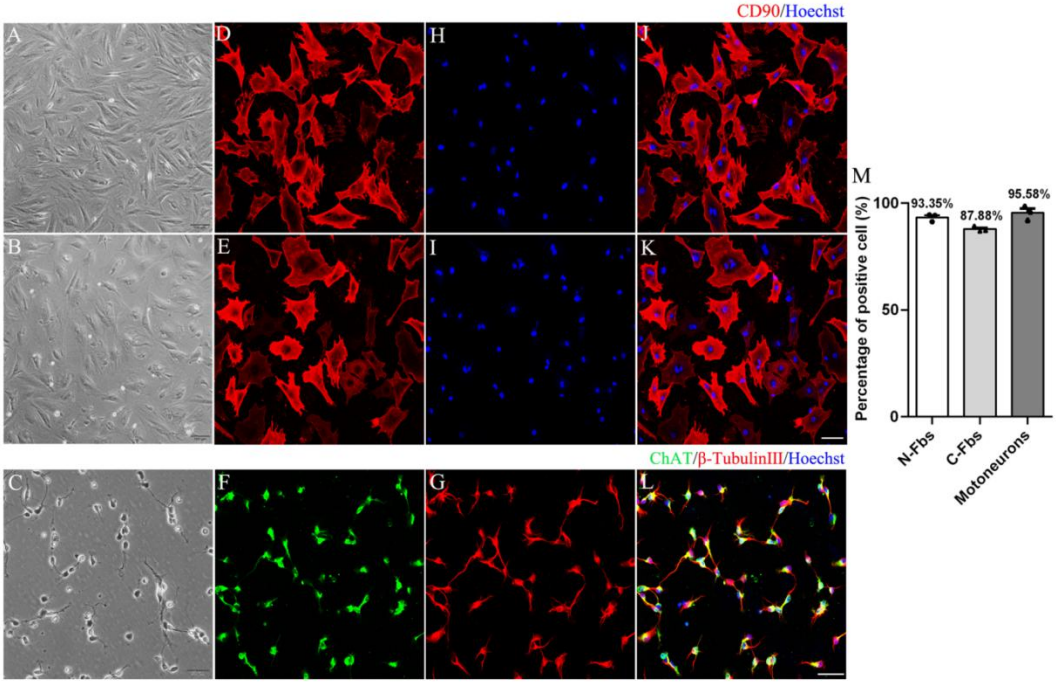

Additional Figure 2 Identification of N-Fbs, C-Fbs, and motoneurons.

(A-C) Phase-contrast micrograph showing typical cell morphology of primary cultured N-Fbs (A), C-Fbs (B) and motoneurons (C). The N-Fbs and C-Fbs exhibited larger, flat and irregular shape, the cell bodies of motoneuron were round or oval, with more neurites. (D-L) Fluorescence microscope photograph of cultured N-Fbs (D, H, J), C-Fbs (E, I, K) and motoneurons (F, G, L) following immunostaining with antibody against CD90 (red, Cy3), ChAT (green, Alexa Fluor 488), β-tubulin III (red, Cy3) respectively, and Hoechst 33342 (blue) nucleus staining. (C, G, M) The merge. Scale bars: 100 μm in A-I, K-M; 50 μm in J. (M) Percentage of CD90 positive cells in N-Fbs or C-Fbs and percentage of ChAT, β-Tubulin III positive cells in motoneurons. Data are expressed as mean ± SEM. The experiments were repeated by three times. C-Fbs: Cardiac fibroblasts; ChAT: choline acetyltransferase; N-Fbs: nerve fibroblasts.

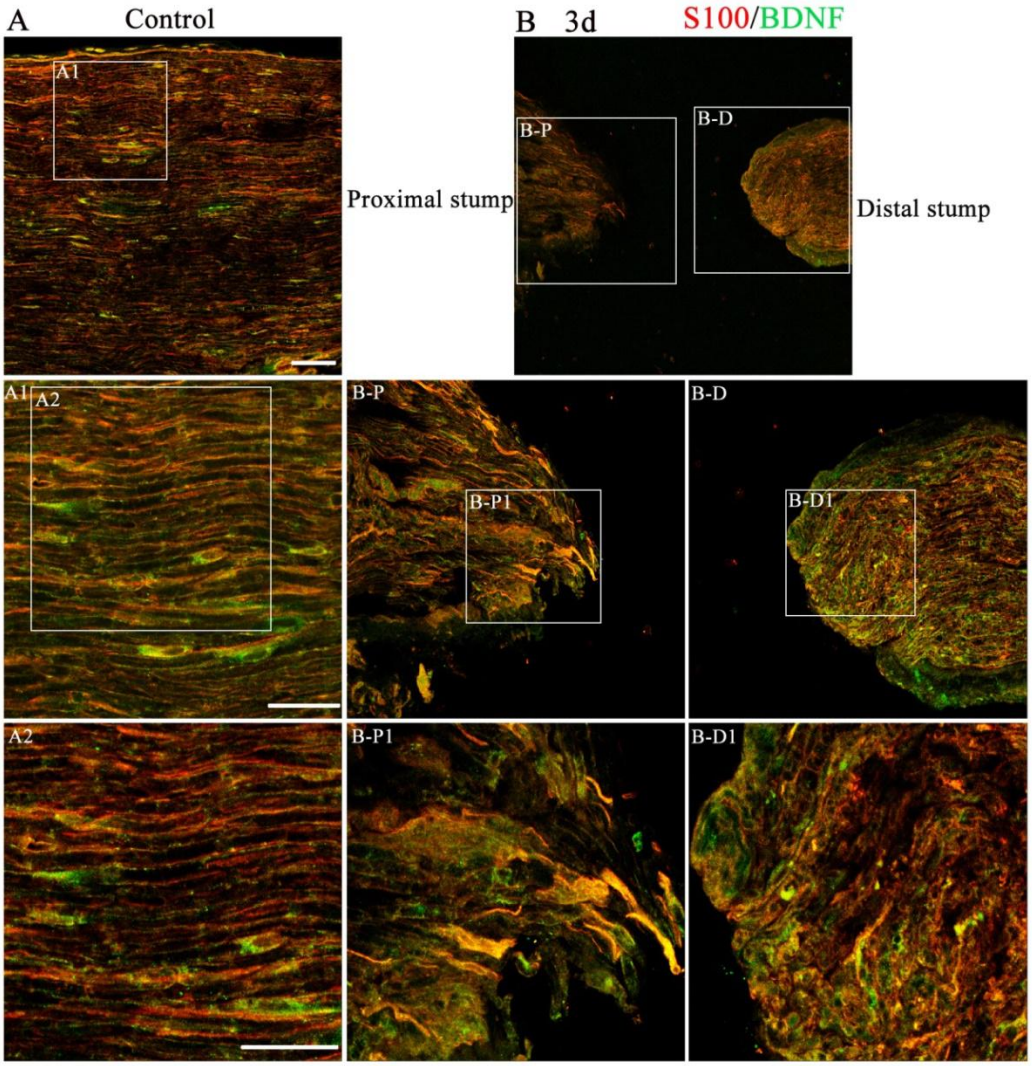

Additional Figure 3 BDNF positive expression in SCs at the injured or normal sciatic nerve site of rats.
(A) BDNF (green, Alexa Fluor 488) positive expression in SCs (marked by S100, red, Cy3) at the normal nerve site (control). (B) BDNF expression in SCs at the injured nerve site at 3 days post-injury. Images in the lower panel are high magnifications of boxed areas in the upper panel. At 3 days after transection, the expression of BDNF in the proximal stump and distal stump was higher than that of the control group. Scale bars: 50 μm. P and D stand for the proximal and distal stump respectively. BDNF: Brain-derived neurotrophic factor; SC: Schwann cell.

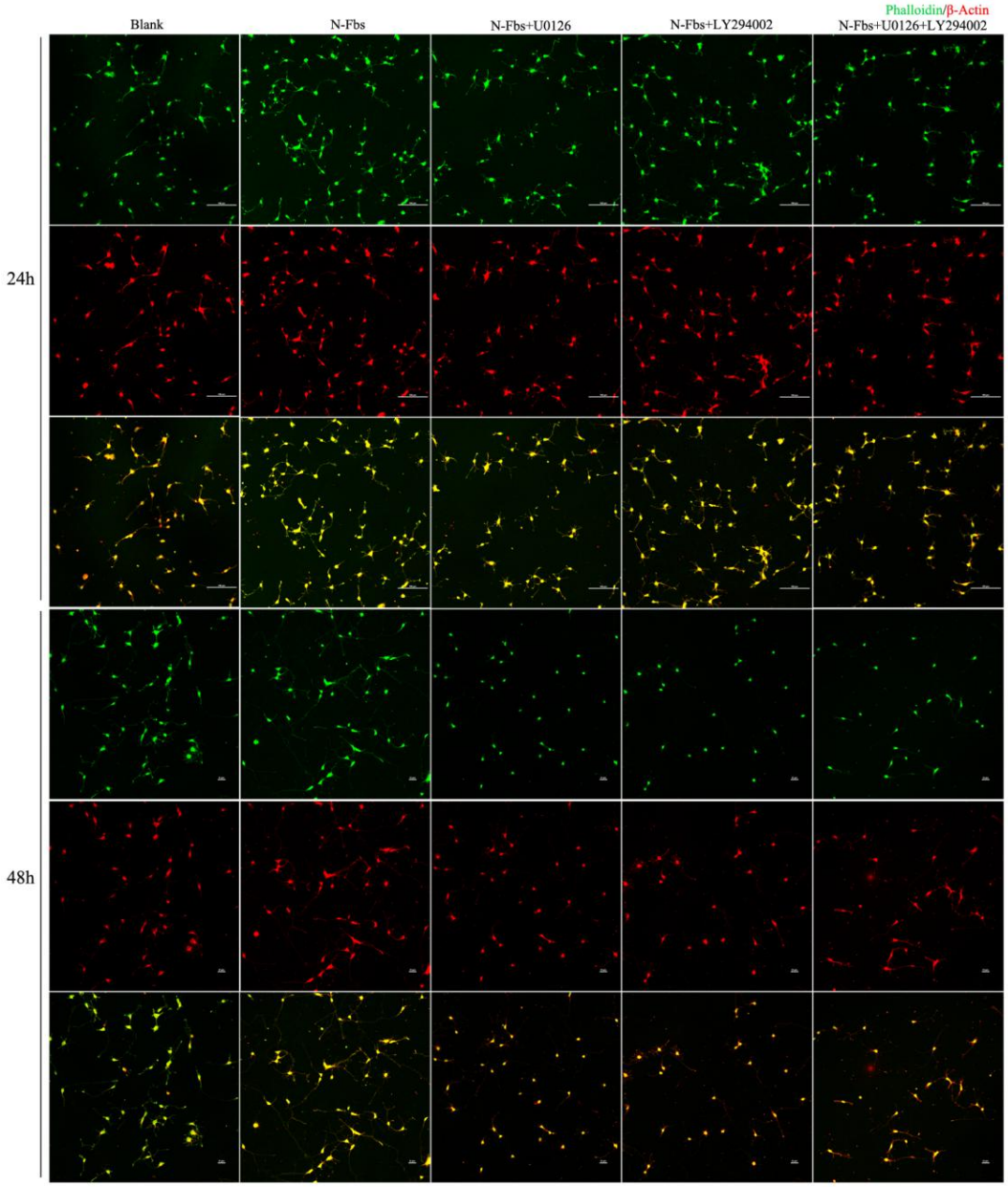

Additional Figure 4 Lower-magnification image of Figure 8A.

The immunostaining showed that after co-culture of motoneurons with N-Fbs for 24 or 48 hours, the expressions of F-actin (marked by phalloidin) and β-actin in motoneurons were significantly increased, but the increase could be inhibited by U0126 and MK2206. Phalloidin (green, Alexa Fluor 488) and β-actin (red, Cy3) immunostaining of motoneurons after co-culture with N-Fbs, N-Fbs + U0126, N-Fbs + MK2206, or N-Fbs + U0126 + MK2206 for 24 or 48 hours respectively. Scale bar: 100 μm. MK2206: Potent AKT inhibitor; N-Fbs: nerve fibroblasts; N-Fbs-CM: nerve fibroblasts conditioned medium; U0126: potent ERK inhibitor.

Additional Table 2 The primer sequences for quantitative real-time polymerase chain reaction

Gene name	Gene sequence (5' to 3')	Product length (bp)
Gapdh	Forward: TCT CTG CTC CTC CCT GTT C	87
	Reverse: ACA CCG ACC TTC ACC ATC T	
Ngfr	Forward: GAC AGT GCA ACG CTT GAT G	142p
	Reverse: GAA TGT GGG ACA GGA CAG G	
Nectin1	Forward: TGG GCT AAG AGA GGG CAT A	144
	Reverse: GGA GGC AGG AAG GTG AAG	
Dlx5	Forward: GCT CAT CCC GCT CTC TC	112
	Reverse: CTG GCT GCA CTT GGG TA	
Bdnf	Forward: TTC TGT AAT CGC CAA GGT G	239
	Reverse:TTT GCT CAG TGG ATC GC	
Fez1	Forward: CAG ACC TTT GGC TCC TCA	146
	Reverse: GGC ACC TTC TCG TTA TCC T	
Reln	Forward: CAC CTG CCT ACA ACA AAC C	104
	Reverse: AAA ATC ACC TGA CCC CTG T	
Epha3	Forward: GGG CAA GAG GCA CAA AT	150
	Reverse: CAC CAG AGA TGG AGA AGG A	
Serpine2	Forward: GAA GAT GGG ACC AAA GCC	102
	Reverse: TCG GAT GCA GAA CAG GA	
Wnt5a	Forward: CGC TGC TGG AGT GGT AA	103
	Reverse: GTC CCG AGG TAA GTC CTT G	

Bdnf: brain-derived neurotrophic factor; Dlx5: distal-less homeobox 5; Epha3: Eph receptor A3; Fez1: fasciculation and elongation protein zeta 1; Gapdh: glyceraldehyde triphosphate dehydrogenase; Nectin1: nectin cell adhesion molecule 1; Ngfr: nerve growth factor receptor; Reln: reelin; Serpine2: serpin family E member 2; Wnt5a: wnt family member 5A.